Article ID: 1006-8775(2016) 02-0182-09

CONVECTIVE–STRATIFORM RAINFALL PARTITION BY RADIANCE–DERIVED CLOUD CONTENT: A MODELING STUDY

SHEN Xin-yong (沈新勇)[1], MEI Hai-xia (梅海霞)[1], QING Tao (庆 涛)[1], Xiaofan LI (李小凡)[2]
(1. Key Laboratory of Meteorological Disaster, Ministry of Education / Joint International Research Laboratory of Climate and Environment Change / Collaborative Innovation Center on Forecast and Evaluation of Meteorological Disasters, Nanjing University of Information Science and Technology, Nanjing 210044 China; 2. School of Earth Sciences, Zhejiang University, Hangzhou 310027 China)

Abstract: A new scheme that separates convective-stratiform rainfall is developed using threshold values of liquid water path (LWP) and ice water path (IWP). These cloud contents can be predicted with radiances at the Advanced Microwave Sounding Unit (AMSU) channels (23.8, 31.4, 89, and 150 GHz) through linear regression models. The scheme is demonstrated by an analysis of a two-dimensional cloud resolving model simulation that is imposed by a forcing derived from the Tropical Ocean Global Atmosphere Coupled Ocean-Atmosphere Response Experiment (TOGA COARE). The rainfall is considered convective if associated LWP is larger than 1.91 mm or IWP is larger than 1.70 mm. Otherwise, the rainfall is stratiform. The analysis of surface rainfall budget demonstrates that this new scheme is physically meaningful.

Key words: cloud-resolving model simulation; radiance transfer model; radiance temperature simulation; convective-stratiform rainfall partition; liquid water path; ice water path
CLC number: P435 **Document code:** A
doi: 10.16555/j.1006-8775.2016.02.008

1 INTRODUCTION

Precipitation is one of the most important meteorological quantities for scientific research and operational forecast. Better understanding of precipitation processes from scientific research leads to the improvement of operational forecast of precipitation. Precipitation can be partitioned into convective and stratiform components due to different dynamic, cloud microphysical, and water vapor processes. Convective precipitation is stronger than stratiform precipitation in terms of rainfall intensity and amount. Convective precipitation is associated with larger horizontal gradients in radar reflectivity than stratiform precipitation. Gao and Li[1] found that ascending motions associated with convective precipitation appear through the entire troposphere whereas those associated with stratiform precipitation only occurs in the upper troposphere, but the former is much stronger than the latter. Dominant cloud microphysical processes are the accretion of cloud water by raindrops via collisions in strong updraft cores in convective precipitation and the vapor deposition on ice particles in stratiform precipitation (Houghton[2]). Cui and Li[3] revealed that convective precipitation is primarily associated with water vapor convergence over convective regions whereas stratiform precipitation is primarily related to local atmospheric drying and transport of hydrometeor concentration from convective regions to stratiform regions.

Most of methods for partitioning convective-stratiform rainfall have been developed primarily based on differences in reflectivity in observational radar data (Houze [4]; Steiner and Houze [5]; Steiner et al.[6]; Rosenfeld et al.[7]) and simulated surface rain rate (Tao et al.[8]; Sui et al.[9]; Tao et al.[10]) between the grid and its neighbors. For instance, in the separation scheme of Churchill and Houze [4], the cores of convective cells are first assigned to those data points in the radar reflectivity field that have rain rates twice as high as the average taken over the surrounding 400 km^2. These convective cores and the surrounding 150 km^2 of area are identified as convective precipitation. In addition, any radar echo of larger than 40 dBz (10 mm h^{-1}) is considered convective precipitation. These partition schemes basically require information from surrounding areas.

Sui et al. [11] developed a new partition method based on threshold values of the cloud content in terms of mass-integrated maxing ratios of ice hydrometeors (ice water path, IWP) and water hydrometeors (liquid water path, LWP), and their ratio (cloud ratio, IWP/LWP). In their scheme, rainfall can be designated

Received 2014-01-09; **Revised** 2015-12-04; **Accepted** 2016-04-15
Foundation item: National Key Basic Research and Development Project of China (2013CB430103, 2015CB453201); National Natural Science Foundation of China (41475039, 41375058, 41530427); Priority Academic Program Development of Jiangsu Higher Education Institutions (PAPD)
Biography: SHEN Xin-yong, Professor, primarily undertaking research on mesoscale meteorology, cloud and precipitation physics.
Corresponding author: SHEN Xin-yong, e-mail: sxydr@126.com

convective when the corresponding value of cloud ratio is smaller than 0.2 or the value of IWP is larger than 2.55 mm. The remaining grids are classified as mixed and stratiform when the corresponding range of cloud ratio is 0.2–1.0, and greater than 1, respectively. The cloud ratio, the main parameter in this scheme, can be a singularity when the water clouds are absent.

In this study, a new convective-stratiform rainfall separation scheme is proposed based on threshold values of LWP and IWP. The rainfall-related cloud contents are derived from simulated radiances at selected microwave channels through linear regression models. We will show that the new scheme has the advantage of Sui scheme that is not based on the information from the surrounding grids. The new scheme does not have the disadvantage of Sui scheme that is invalid in the absence of ice clouds. The models and experiment are briefly described in the next section. Results are presented in section 3. A summary is given in section 4.

2 MODEL AND EXPERIMENT

The cloud-resolving model was originally developed by Soong and Ogura[12], Soong and Tao[13] and Tao and Simpson[14], and further modified by Li et al.[15]. The 2D-version of the model used in this study has cyclic lateral boundary conditions and prognostic equations for potential temperature, specific humidity, mixing ratios of cloud water, rain, cloud ice, snow, and graupel, and perturbation horizontal and vertical components of wind. The model includes prognostic cloud microphysical parameterization schemes (Lin et al.[16]; Rutledge and Hobbs [17]; Rutledge and Hobbs [18]; Tao and Simpson[19]; Krueger et al.[20]) and interactive radiative parameterization schemes (Chou et al.[21-23]). The model uses a horizontal domain of 768 km, a horizontal grid resolution of 1.5 km, 33 vertical layers, and a time step of 12 s.

The experiment analyzed in this study is conducted with the model forced by the zonally uniform vertical velocity, zonal wind, and thermal and moisture advections, which are derived by Professor Minghua Zhang and his research group at the State University of New York at Stony Brook, based on the 6-hourly TOGA COARE observations within the Intensive Flux Array (IFA) region (Zhang, personal communication, 1999). The calculations are based on the constrained variational method on column-integrated budgets of mass, heat, moisture and momentum proposed by Zhang and Lin[24]. Hourly sea surface temperature (SST) at the Improved Meteorological (IMET) surface mooring buoy (1.75° S, 156°E) (Weller and Anderson[25]) is also imposed in the model. The model is integrated from 0400 LST 19 December 1992 to 0400 LST 9 January 1993 (A total of 21 days). Fig. 1 shows the time-pressure cross section of the large-scale atmospheric vertical velocity, zonal wind, and the time series of SST during the 21-day period. The model simulation data are compared with available observational data in terms of temperature, specific humidity, rain rate, and surface solar radiative and latent heat fluxes [15] and are in-depth examined to study dominant cloud microphysical processes (Li et al.[26, 27]), energetic budget associated with phase difference between convective available potential energy and surface rain rate (Li et al.[28]), surface rainfall processes (Gao et al.[29, 30]; Cui and Li [3]; Gao and Li [31, 32]; Shen et al.[33]), precipitation efficiency (Li et al.[28]; Sui et al.[34, 35]), diurnal variation of rainfall (Gao et al.[36]; Gao and Li[37]), cloud cluster and their merging (Ping et al.[38]), and vorticity vectors (Gao et al.[39, 40]). Xu et al.[41] used the two-dimensional cloud-resolving model to successfully simulate the surface rainfall processes over the Yangtze-Huaihe Rivers valley.

Weng et al.[42] found that the radiances at 23.8 and 31.4 GHz are used to retrieve liquid water path because of their sensitivity to water hydrometeors, whereas the radiances at 89 and 150 GHz are used to retrieve ice water path due to their sensitivity to ice hydrometeors. Radiances in this study are simulated using the version 1 of Joint Center for Satellite Data Assimilation (JCSDA) Community Radiative Transfer Model (CRTM) (Han et al.[43]) and vertical profiles of temperature, specific humidity, mixing ratios and effective radii of cloud water, cloud ice, raindrops, snow, and graupel from the cloud-resolving model simulation. The forward model contains models for calculations of surface emissivity reflectivity over ocean, land, and ice and snow surface, aerosol absorption scattering, cloud absorption scattering, and gaseous absorption, whose outputs are used by tangent linear, adjoint, and K-Maxtrix models to simulate radiances.

The surface rainfall budget can be analyzed using surface rainfall equation derived by Gao et al.[29] and Cui and Li[3]. The surface rainfall equation is written by

$$P_s = Q_{\mathrm{WVT}} + Q_{\mathrm{WVF}} + Q_{\mathrm{WVE}} + Q_{\mathrm{CM}}, \tag{1}$$

$$Q_{\mathrm{WVT}} = -\frac{\partial [q_v]}{\partial t}, \tag{1a}$$

$$Q_{\mathrm{WVF}} = -[\overline{u}^{o}\frac{\partial \overline{q}_v^{\,o}}{\partial x}] - [\overline{w}^{o}\frac{\partial \overline{q}_v}{\partial z}] - [\frac{\partial (u' q_v')}{\partial x}] - [\overline{u}^{o}\frac{\partial q_v}{\partial x}] - [\overline{w}^{o}\frac{\partial q_v}{\partial z}] - [w'\frac{\partial \overline{q}_v}{\partial z}], \tag{1b}$$

$$Q_{\mathrm{WVE}} = E_s, \tag{1c}$$

$$Q_{\mathrm{CM}} = -\frac{\partial [q_5]}{\partial t} - [u\frac{\partial q_5}{\partial x}] - [w\frac{\partial q_5}{\partial z}], \tag{1d}$$

where Q_{WVT} is the local water vapor storage, Q_{WVF} is water vapor convergence, Q_{WVE} is the surface evaporation (E_s); Q_{CM} is hydrometeor convergence minus storage; u and w are zonal and vertical wind components, respectively; a prime denotes a perturbation from the model domain mean; the symbol ^{o} is an imposed forcing; and $[()] = \int_{z_b}^{z_t} \overline{\rho}()dz$, z_t and z_b are the heights of the top and bottom of the model atmosphere respectively.

Following Sui and Li [44], model domain mean bud-

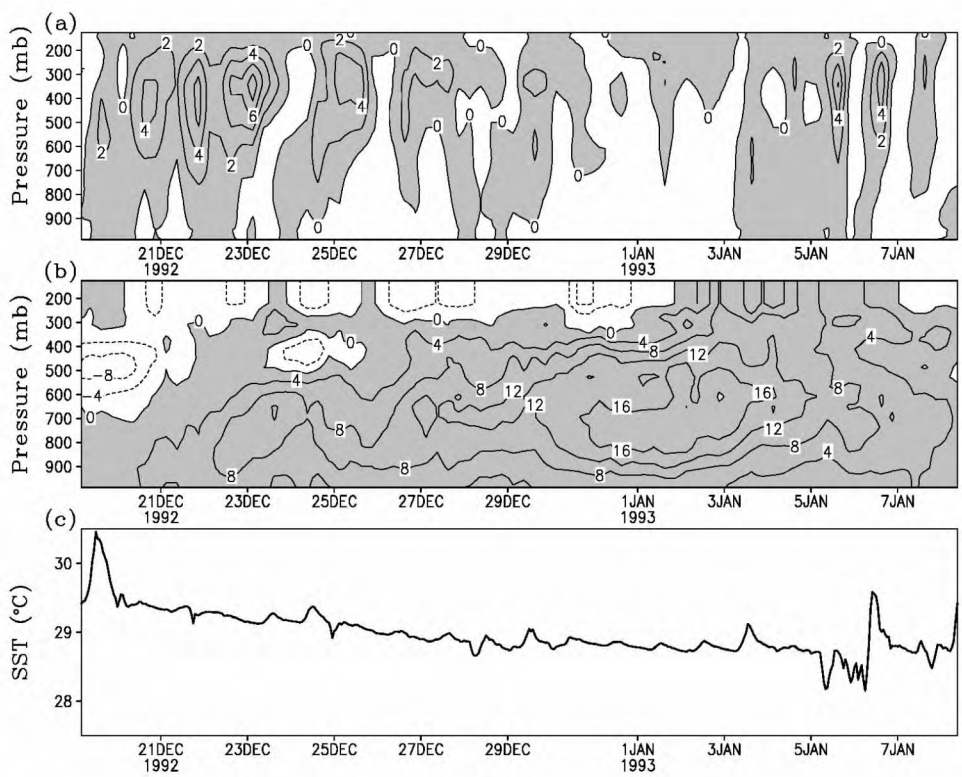

Figure 1. Time-pressure cross section of (a) vertical velocity (cm s^{-1}), (b) zonal wind (m s^{-1}), and the time series of (c) sea surface temperature (℃) derived from observations made in TOGA COARE for 21-day period. Upward motion in (a) and westerly wind in (b) are shaded.

get of LWP tendency is expressed by

$$\frac{\partial \mathrm{LWP}}{\partial t} = -P_S + [P_{\mathrm{CND}}] + C(\mathrm{IWP},\mathrm{LWP}) - [P_{\mathrm{REVP}}], \qquad (2)$$

where

$$C(\mathrm{IWP},\mathrm{LWP}) = -[P_{\mathrm{SACW}}(T<T_o)] - [P_{\mathrm{GACW}}(T<T_o)] + [P_{\mathrm{SMLT}}(T>T_o)] + [P_{\mathrm{GMLT}}(T>T_o)] \qquad (2a)$$

3 RESULTS

Convective rainfall comes primarily from water clouds, and is also from regions in which strong updrafts support large graupels. The averages of LWP and IWP over rainy area during the model integration are 1.37 mm and 0.85 mm, respectively, whereas their standard deviations are 2.14 mm and 1.70 mm, respectively. The threshold of LWP for identification of convective rainfall is larger than its area average, which is mean LWP plus one-fourth of standard deviation (1.91 mm). The threshold of IWP is mean IWP plus a half of standard deviation (1.70 mm).

The AMSU channels at 23.8 GHz and 31.4 GHz are sensitive to water hydrometeors and their radiances are used to retrieve LWP, whereas those at 89 GHz and 150 GHz are sensitive to ice hydrometeors and their radiances are used to retrieve IWP (e.g. Weng et al.[42]). Scatter plots of Ln (SST-T_{b23}) and Ln (SST-T_{b31}) versus LWP and Ln (SST-T_{b89}) and Ln (SST-T_{b150}) versus IWP suggest a first order of approximation of relation between cloud contents and simulated radiances (Fig.2), where SST is sea surface temperature; T_{b23}, T_{b31}, T_{b89}, and T_{b150} are brightness temperatures at 23.8, 31.4, 89, and 150 GHz, respectively. Thus, linear regression equations for LWP and T_{b23} and T_{b31} and IWP and T_{b89} and T_{b150} are written by

$$\mathrm{LWP} = A_{\mathrm{L}} + B_{23}\mathrm{Ln}(\mathrm{SST} - T_{b23}) + B_{31}\mathrm{Ln}(\mathrm{SST} - T_{b31}), \quad (3a)$$

$$\mathrm{IWP} = A_{\mathrm{I}} + B_{89}\mathrm{Ln}(\mathrm{SST} - T_{b89}) + B_{150}\mathrm{Ln}(\mathrm{SST} - T_{b150}), \quad (3b)$$

where A_{L}, B_{23}, and B_{31} are 182.80, 8.47, and −45.22, respectively; A_{I}, B_{89}, and B_{150} are −33.77, −1.01, 12.73, respectively. The linear correlation coefficients for (3a) and (3b) are 0.38 and 0.35, respectively, which are statistically significant. In the new scheme, model grid is considered convective if

$$A_{\mathrm{L}} + B_{23}\mathrm{Ln}(\mathrm{SST} - T_{b23}) + B_{31}\mathrm{Ln}(\mathrm{SST} - T_{b31}) > 1.91 \quad (4a)$$

or

$$A_{\mathrm{I}} + B_{89}\mathrm{Ln}(\mathrm{SST} - T_{b89}) + B_{150}\mathrm{Ln}(\mathrm{SST} - T_{b150}) > 1.70. \quad (4b)$$

Otherwise, it is stratiform.

The vertical profiles of time-mean vertical velocity averaged over stratiform and convective regions in Fig. 3 show similar ascending motions over the two regions above 9 km. The ascending motions increase as the height decreases and reach their maximum around 2.5 km, whereas the ascending motions decrease as the height decreases and the vertical motions become downward around 3 km. The vertical profiles of vertical velocity associated with convective and stratiform rainfall

here are similar to those partitioned by the scheme of Sui et al.[9] (see Fig. 1 in Sui et al.[11]). Thus, convective rainfall is powered by upward motions throughout the troposphere, whereas stratiform rainfall is weaker than convective rainfall due to prevailed downward motions near the surface over stratiform regions. The contoured frequency by altitude diagrams (CFAD) of vertical velocity in the two regions in Fig. 4 reveals a broader distribution of vertical velocity in convective regions than in stratiform regions. The maximum vertical velocity generally is larger than 15 m s^{-1} in convective regions and less than 10 m s^{-1} in stratiform regions. The rainfall for (4a) accounts for 79.2% of convective rainfall, whose upward motions occur throughout the troposphere with the maximum (>50 cm s^{-1}) around 2.5 km (not shown). The rainfall for (4a) contributes 20.8% to convective rainfall. The associated vertical velocity shows upward motions above 5 km and the maximum upward motions (>50 cm s^{-1}) appears around 9 km (not shown), which supports the growth of graupel.

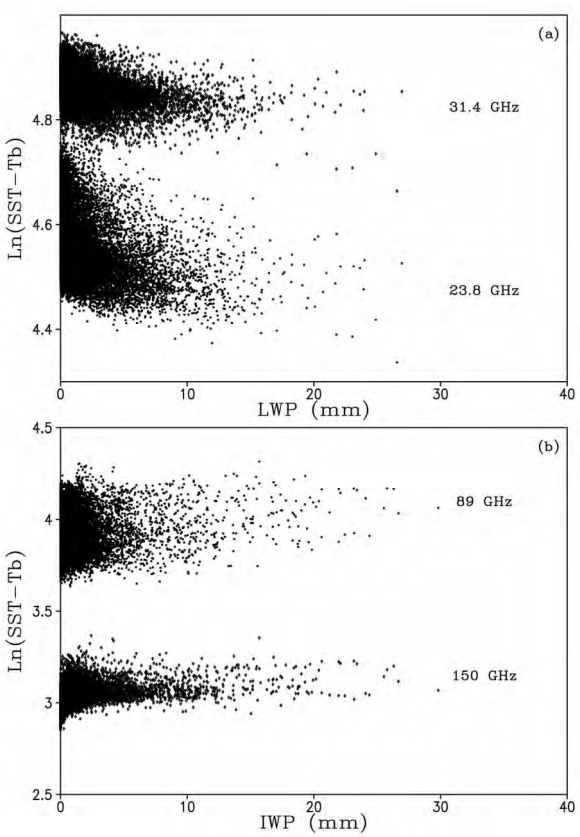

Figure 2. (a) Ln(SST-T_b) with brightness temperature (T_b) at 23.8 and 31.4 GHz versus liquid water path (LWP), and (b) Ln (SST-T_b) with brightness temperature at 89 and 150 GHz versus ice water path (IWP). Unit for IWP and LWP is mm.

The mean cloud microphysical budgets over convective and stratiform regions in Fig.5 show differences. LWP is 140% larger than IWP over convective regions, whereas it is 28% larger than IWP over stratiform regions. The vapor condensation and deposition rates (P_{CND}+P_{DEP}+P_{SDEP}+P_{GDEP}) over convective regions are

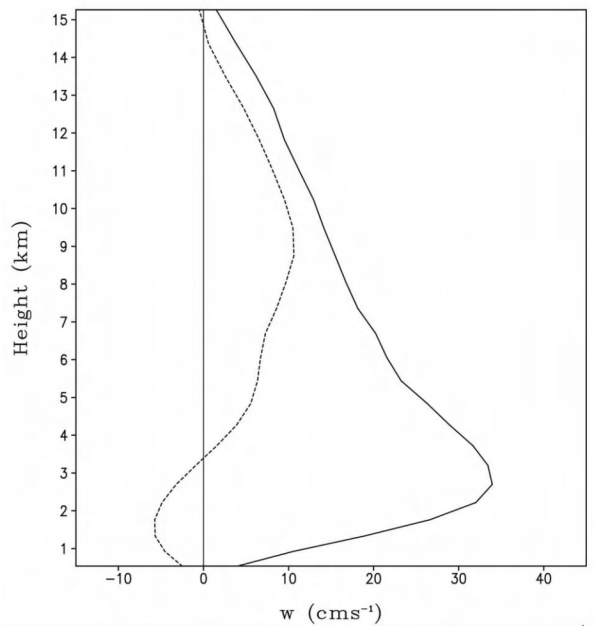

Figure 3. Vertical profiles of vertical velocity (cm s^{-1}) averaged in stratiform (dash) and convective (solid) regions.

almost five times as larger as those over straitofrm regions. As a result, microphysics-produced rain rate (*Sqr*) over convective regions is about five times as large as that over stratiform regions. Microphysics-produced rain rate is lower than surface rain rate over stratiform regions, whereas it is higher than surface rain rate over convective regions; indicating the transport of hydrometeor concentration from convective regions to stratiform regions. Over convective regions, the collection rate of cloud water by rain (P_{RACW}) is 237.55% higher than the melting rate of graupel to rain (P_{GMLT}). In contrast, the two rates are similar over stratiform regions. The conversion rate from *IWP* to *LWP* [P_{GMLT}+P_{SMLT}−P_{SACW}−P_{GACW} (T<T_o)] over stratiform regions (0.80 mm h^{-1}) is twice as large as that over convective regions (0.37 mm h^{-1}). The microphysical processes and their parameterization schemes shown in Fig. 5 are listed in Table 1, which are from Lin et al.[16] (LFO), Rutledge and Hobbs [17, 18] (RH83, RH84), Tao et al.[19] (TSM), and Krueger et al.[20] (KFLC). T is air temperature and T_o=0℃. A complete list of microphysical processes and their parameterization schemes used in the model can be found in Gao and Li[32].

Stratiform rainfall is associated with local atmospheric drying over stratiform regions and the transport of hydrometeor concentration from convective regions to stratiform regions, while the water vapor divergence is prevailed over stratiform regions (Table 2). Convective rainfall is primarily from water vapor convergence over convective regions, while the transport of hydrometeor concentration from convective regions to stratiform regions leads to local atmospheric drying over convective regions.

Since the LWP is primarily used to detect convec-

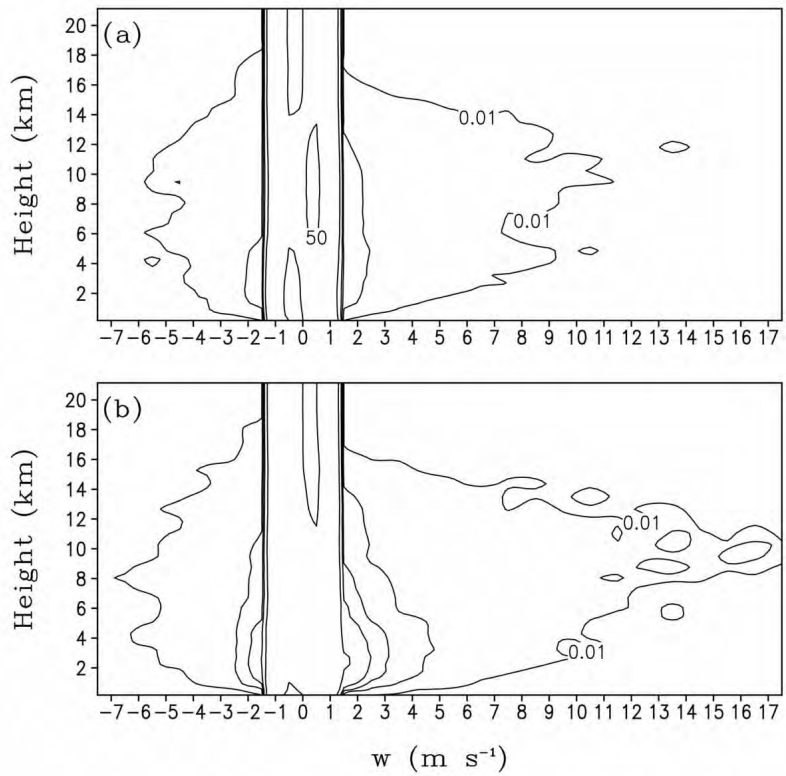

Figure 4. CFAD of vertical velocity (m s^{-1}) for (a) stratiform and (b) convective regions. Contour intervals are 0.01%, 1%, 3%, 5%, 10%, and 50%, respectively.

tive rainfall, the relation between the fractional coverage of convective rainfall and model domain mean LWP is examined in Fig. 6. The fractional coverage of convective rainfall increases as the mean LWP increases. Their linear correlation coefficient is 0.75 and this correlation is statistically significant. Since the fractional coverage of convective rainfall is highly correlated with the mean LWP, the tendency of LWP may be the indicative of the change of fractional coverage of convective rainfall. Thus, the mean LWP tendency is analyzed.

The vapor condensation and conversion from ice hydrometeors to water hydrometeors cause the increase of LWP, whereas the rainfall and evaporation of rain yield the decrease of LWP (Table 3). The conversion from IWP to LWP is very important in producing the positive LWP tendency since the vapor condensation alone cannot overcome the loss of LWP due to rainfall and evaporation of rain. The negative LWP tendency is primarily associated the large decrease of vapor condensation rate, while it is also contributed to by the slowdown of conversion from IWP to LWP.

4 SUMMARY

A new method to partition tropical rainfall into the stratiform and convective components using radiances at four AMSU channels 23.8, 31.4, 89, and 150 GHz. The outputs from a two-dimensional cloud resolving model simulation with the imposed forcing from the Tropical Ocean Global Atmosphere Coupled Ocean-Atmosphere Response Experiment (TOGA COARE) are used to simulate radiances with the version 1 of community radiative transfer model developed by the Joint Center for Satellite Data Assimilation, USA. The radiances at 23.8 and 31.4 GHz predict LWP, whereas those at 89 and 150 GHz predict IWP through statistically significant linear regression relations. In this new convective-stratiform rainfall separation scheme, the rainfall is considered convective if radiance-derived LWP is larger than 1.91 mm (mean plus one fourth of standard deviation) or radiance-derived IWP is larger than 1.70 mm (mean plus a half of standard deviation).

The averaged data partitioned with this new scheme show that maximum upward motions over convective regions occur in the lower troposphere whereas the upward motions appear in the upper troposphere and downward motions occur in the lower troposphere. The maximum upward motions are larger than 15 m s^{-1} over convective regions but they are generally smaller than 10 m s^{-1}. The analysis of cloud microphysical budgets reveals that the primarily microphysical process related to convective rainfall is the collection of cloud water by rain and the main microphysical processes associated with stratiform rainfall are the melting of graupel to rain and collection of cloud water by rain. The surface rainfall budgets show that convective rainfall is primarily associated with water vapor convergence over convec-

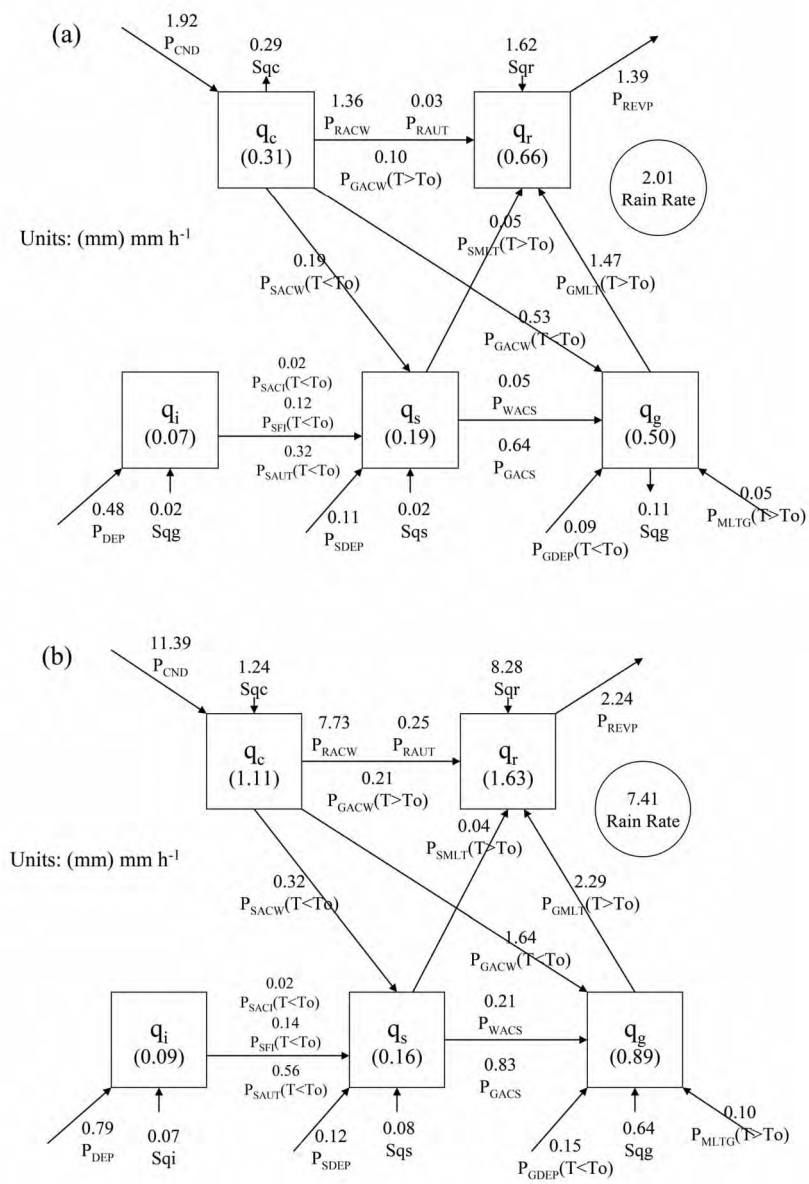

Figure 5. Cloud microphysics budgets averaged in (a) stratiform, and (b) convective region. Units for cloud hydrometeors and conversions are mm and mm h^{-1}, respectively.

tive regions, whereas stratiform rainfall is mainly from local atmospheric drying over stratiform regions and the transport of hydrometeor from convective regions to stratiform regions.

The fractional coverage of convective rainfall links to model domain mean LWP. Their statistically significant linear correlation shows that the fractional coverage of convective rainfall increases as the mean LWP increases. Thus, the budget of LWP tendency is analyzed. The vapor condensation and conversion from IWP to LWP make rainfall system more convective, while the precipitation and evaporation of rain make the system less convective. The change of fractional coverage of convective rainfall depends on the relative importance of these processes.

The advantages for the new scheme are: (1) the new scheme does not require information from neigh-

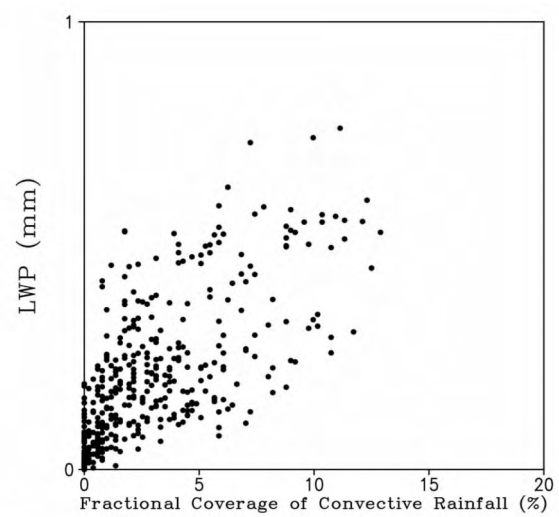

Figure 6. Scatter plotting of model domain mean LWP (mm) versus fractional coverage of convective rainfall (%).

Table 1. List of microphysical processes and their parameterization schemes shown in Fig. 5.

Notation	Description	Scheme
P_{MLTG}	Growth of vapor by evaporation of liquid from graupel surface	RH84
P_{REVP}	Growth of vapor by evaporation of raindrops	RH83
P_{CND}	Growth of cloud water by the condensation of supersaturated vapor	TSM
P_{GMLT}	Growth of raindrops by melting of graupel	RH84
P_{SMLT}	Growth of raindrops by melting of snow	RH83
P_{RACW}	Growth of raindrops by the collection of cloud water	RH83
P_{RAUT}	Growth of raindrops by the autoconversion of cloud water	LFO
P_{DEP}	Growth of cloud ice by the deposition of supersaturated vapor	TSM
P_{SAUT}	Growth of snow by the conversion of cloud ice	RH83
P_{SACI}	Growth of snow by the collection of cloud ice	RH83
P_{SACW}	Growth of snow by the accretion of cloud water	RH83
P_{SFI}	Depositional growth of snow from cloud ice	KFLC
P_{SDEP}	Growth of snow by the deposition of vapor	RH83
P_{GACS}	Growth of graupel by the accretion of snow	RH84
P_{GACW}	Growth of graupel by the accretion of cloud water	RH84
P_{WACS}	Growth of graupel by the riming of snow	RH84
P_{GDEP}	Growth of graupel by the deposition of vapor	RH84
Sqc	$Sqc= PCND-PRACW-PRAUT-PGACW$	
Sqr	$PRACW+PRAUT+PGACW(T>To)+PSMLT+PGMLT-PREVP$	
Sqi	$Sqi=PDEP-PSFI-PSAUT-PSACI$	
Sqs	$Sqs= PSDEP+PSFI+PSAUT+PSACI-PSMLT-PWACS-PGACS$	
Sqg	$Sqg= PGDEP+PWACS+PGACS+PGACW(T<To)-PGMLT+PMLTG$	

Table 2. Time means of PS , QWVT, QWVF, QWVE , and QCM averaged over stratiform and convective regions. Unit is mm h^{-1}.

Notation	Stratiform regions	Convective regions
P_S	2.01	7.41
Q_{WVT}	1.80	3.04
Q_{WVF}	−0.84	6.51
Q_{WVE}	0.20	0.55
Q_{CM}	0.86	−2.69

Table 3. Model domain means of positive and negative LWP tendencies and associated tendency budgets. Unit is mm h^{-1}.

	Positive LWP tendency	Negative LWP tendency
$\partial LWP/\partial t$	0.09	−0.08
P_{CND}	0.55	0.41
$-P_S$	−0.35	−0.37
$-P_{REVP}$	−0.24	−0.20
$C(IWP,LWP)$	0.13	0.08

boring grids. In contrast, most partitioning method needs this information (e.g., Sui et al.[9]); (2) the new scheme works but the scheme of Sui et al.[11] does not work when the water clouds are absent; (3) the convective-stratiform rainfall can be determined by either radiances at selected AMSU channels or LWP and IWP.

Caution should be exercised since the scheme is only tested in a two-dimensional model framework. A further examination of this new scheme with three-dimensional model simulation data and observational data is necessary to validate the separation scheme.

Acknowledgement: Authors thank Prof. M. Zhang at the State University of New York, Stony Brook for allowing us to use his TOGA COARE forcing data, Drs. Q. Liu and Y. Han at the Joint Center for Satellite Data Assimilation, Camp Springs, Maryland for the version 1 of community radiative transfer model.

REFERENCES:

[1] GAO S, LI X. Responses of tropical deep convective precipitation systems and their associated convective and stratiform regions to the large-scale forcing [J]. Quart J Roy Meteorol Soc, 2008, 134(637): 2 127-2 141.

[2] HOUGHTON H G. On precipitation mechanisms and their artificial modification [J]. J Appl Meteorol, 1968, 7(5): 851-859.

[3] CUI X, LI X. Role of surface evaporation in surface rainfall processes [J]. J Geophys Res, 2006, 111, D17112, doi: 10.1029/2005JD006876.

[4] HOUZE R A JR. A climatological study of vertical transports by cumulus-scale convection [J]. J Atmos Sci, 1973, 30(6): 1 112-1 123.

[5] STEINER M, HOUZE R A JR. Three-dimensional validation at TRMM ground truth sites: Some early results from Darwin, Australia [C]// Preprints, 26th Int Conf on Radar Meteorology, Norman, OK, Amer Meteorol Soc, 1993: 417-420.

[6] STEINER M, HOUZE R A JR, YUTER S E. Climatological characterization of three-dimensional storm structure from operational radar and rain gauge data [J]. J Appl Meteorol, 1995, 34(9): 1 978-2 007.

[7] ROSENFELD D, AMITAI E, WOLFF D B. Classification of rain regimes by the three-dimensional properties of re-

flectivity fields [J]. J Appl Meteorol, 1995, 34(1): 198-211.
[8] TAO W K, SIMPSON J, MCCUMBER M. An ice-water saturation adjustment [J]. Mon Wea Rev, 1989, 117(1): 231-235.
[9] SUI C H, LAU K M, TAO W K, et al. The tropical water and energy cycles in a cumulus ensemble model. Part I: Equilibrium climate [J]. J Atmos Sci, 1994, 51(5): 711-728.
[10] TAO W K, LANG S, SIMPSON J, et al. Vertical profiles of latent heat release and their retrieval for TOGA COARE convective systems using a cloud resolving model, SSM/I, and ship-borne radar data [J]. J Meteorol Soc Japan, 2000, 78(4): 333-355.
[11] SUI C H, TSAY C T, LI X. Convective stratiform rainfall separation by cloud content [J]. J Geophys Res, 2007, 112: D14213, doi:10.1029/2006JD008082.
[12] SOONG S T, OGURA Y. Response of tradewind cumuli to large-scale processes [J]. J Atmos Sci, 1980, 37(9): 2 035-2 050.
[13] SOONG S T, TAO W K. Response of deep tropical cumulus clouds to Mesoscale processes [J]. J Atmos Sci, 1980, 37(9): 2 016-2 034.
[14] TAO W K, SIMPSON J. The Goddard Cumulus Ensemble model. Part I: Model description [J]. Terr Atmos Oceanic Sci, 1993, 4(1): 35-72.
[15] LI X, SUI C H, LAU K M, et al. Large-scale forcing and cloud-radiation interaction in the tropical deep convective regime [J]. J Atmos Sci, 1999, 56(17): 3 028-3 042.
[16] LIN Y L, FARLEY R D, ORVILLE H D. Bulk parameterization of the snow field in a cloud model [J]. J Climate Appl Meteorol, 1983, 22(6): 1 065-1 092.
[17] RUTLEDGE S A, HOBBS P V. The mesoscale and microscale structure and organization of clouds and precipitation in midlatitude cyclones. Part VIII: A model for the "seeder-feeder" process in warm-frontal rainbands [J]. J Atmos Sci, 1983, 40(5): 1 185-1 206.
[18] RUTLEDGE S A, HOBBS P V. The mesoscale and microscale structure and organization of clouds and precipitation in midlatitude cyclones. Part XII: A diagnostic modeling study of precipitation development in narrow cold-frontal rainbands [J]. J Atmos Sci, 1984, 41(20): 2 949-2 972.
[19] TAO W K, SIMPSON J. Modeling study of a tropical squall-type convective line [J]. J Atmos Sci, 1989, 46(2): 177-202.
[20] KRUEGER S K, FU Q, LIOU K N, et al. Improvement of an ice-phase microphysics parameterization for use in numerical simulations of tropical convection [J]. J Appl Meteorol, 1995, 34(1): 281-287.
[21] CHOU M D, SUAREZ M J, HO C H, et al. Parameterizations for cloud overlapping and shortwave single scattering properties for use in general circulation and cloud ensemble models [J]. J Atmos Sci, 1998, 55(2): 201-214.
[22] CHOU M D, KRATZD P, RIDGWAYW. Infrared radiation parameterization in numerical climate models [J]. J Climate, 1991, 4(4): 424-437.
[23] CHOU M D, SUAREZM J. An efficient thermal infrared radiation parameterization for use in general circulation model [Z]. NASA TechMemo, 1994, 104606, 3: 85. [Available from NASA/Goddard Space Flight Center, Code 913, Greenbelt, MD 20771.]
[24] ZHANG M H, LIN J L. Constrained variational analysis of sounding data based on column-integrated budgets of mass, heat, moisture, and momentum: Approach and application to ARM measurements [J]. J Atmos Sci, 1997, 54(7): 1 503-1 524.
[25] WELLER R A, ANDERSON S P. Surface meteorology and air-sea fluxes in the western equatorial Pacific warm pool during TOGA COARE [J]. J Climate, 1996, 9(7): 1 959-1 990.
[26] LI X, SUI C H, LAU K M. Dominant cloud microphysical processes in a tropical oceanic convective system: A 2-D cloud resolving modeling study [J]. Mon Wea Rev, 2002, 130(10): 2 481-2 491.
[27] LI X, SUI C H, LAU K M, et al. Tropical convective responses to microphysical and radiative processes: A sensitivity study with a 2D cloud resolving model [J]. Meteorol Atmos Phys, 2005, 90(3-4): 245-259.
[28] LI X, SUI C H, LAU K M. Interactions between tropical convection and its environment: An energetics analysis of a 2D cloud resolving simulation [J]. J Atmos Sci, 2002, 59(10): 1 712-1 722.
[29] GAO S, CUI X, ZHOU Y, et al. Surface rainfall processes as simulated in a cloud resolving model [J]. J Geophys Res, 2005, 110: D10202, doi:10.1029/2004JD005467.
[30] GAO S, RAN L, LI X. Impacts of ice microphysics on rainfall and thermodynamic processes in the tropical deep convective regime: A 2D cloud-resolving modeling study [J]. Mon Wea Rev, 2006, 134(10): 3 015-3 024.
[31] GAO S, LI X. Cloud-resolving modeling of convective processes [M]. Springer, Dordrecht, 2008: 0-206.
[32] GAO S, LI X. Effects of time-dependent large-scale forcing, solar zenith angle, and sea surface temperature on time-mean tropical rainfall processes [J]. Meteorol Atmos Phys, 2010, 106(1-2): 95-105.
[33] SHEN X, WANG Y, ZHANG N, et al. Roles of large-scale forcing, thermodynamics, and cloud microphysics in tropical precipitation processes [J]. Atmos Res, 2010, 97(3): 371-384.
[34] SUI C H, LI X, YANG M J. Estimation of oceanic precipitation efficiency in cloud models [J]. J Atmos Sci, 2005, 62(12): 4 358-4 370.
[35] SUI C H, LI X, YANG M J. On the definition of precipitation efficiency [J]. J Atmos Sci, 2007, 64(12): 4 506-4 513.
[36] GAO S, CUI X, LI X. A modeling study of diurnal rainfall variations during the 21-day period of TOGA COARE [J]. Adv Atmos Sci, 2009, 26(5): 895-905.
[37] GAO S, LI X. Precipitation equations and their applications to the analysis of diurnal variation of tropical oceanic rainfall [J]. J Geophys Res, 2010, doi: 10.1029/2009JD012452.
[38] PING F, LUO Z, LI X. Kinematics, Cloud microphysics, and spatial structures of tropical cloud clusters: A two-dimensional cloud-resolving modeling study [J]. Atmos Res, 2008, 88(3-4): 323-336.
[39] GAO S, PING F, LI X, et al. A convective vorticity vector associated with tropical convection: A two-dimensional cloud-resolving modeling study [J]. J Geophys Res, 2004, 109: D14106, doi:10.1029/2004JD004807.
[40] GAO S, CUI X, ZHOU Y, et al. A modeling study of moist and dynamic vorticity vectors associated with two-dimensional tropical convection [J]. J Geophys Res, 2005, 110: D17104, doi:10.1029/2004JD005675.
[41] XU Feng-wen, CUI Xiao-peng, XU Xiao-feng, et al. A

cloud-resolving modeling study of the surface rainfall processes in the Jiang-Huai valley during July 2007 II: Diagnostic analysis of the simulated surface rainfall processes [J]. J Trop Meteorol, 2011, 27 (3): 365-372 (in Chinese).

[42] WENG F, ZHAOL, POEG, et al. AMSU cloud and precipitation algorithms [J]. Radio Sci, 2003, 38: 8068, doi: 10.1029/2002RS002679.

[43] HAN Y, VAN DELST P, LIU Q, et al. JCSDA Community Radiative Transfer Model (CRTM)-Version 1 [R]. NOAA Technical Report NESDES 122, 2006: 33.

[44] SUI C H, LI X. A tendency of cloud ratio associated with the development of tropical water and ice clouds [J]. Terr Atmos Ocean Sci, 2005, 16(2): 419-434.

Citation: SHEN Xin-yong, MEI Hai-xia, QING Tao et al. Convective-stratiform rainfall partition by radiance-derived cloud content: A modeling study [J]. J Trop Meteorol, 2016, 22(2): 182-190.